

# We are IntechOpen, the world's leading publisher of Open Access books Built by scientists, for scientists

6,900

Open access books available

185,000

International authors and editors

200M

Downloads

Our authors are among the

154

Countries delivered to

TOP 1%

most cited scientists

12.2%

Contributors from top 500 universities



WEB OF SCIENCE™

Selection of our books indexed in the Book Citation Index  
in Web of Science™ Core Collection (BKCI)

Interested in publishing with us?  
Contact [book.department@intechopen.com](mailto:book.department@intechopen.com)

Numbers displayed above are based on latest data collected.  
For more information visit [www.intechopen.com](http://www.intechopen.com)



## Hybrid Materials Based on Zn-Al Alloys

G. Torres-Villaseñor and E. Martínez-Flores

*Instituto de Investigaciones en Materiales, Universidad Nacional Autónoma de México*

*Facultad de Ingeniería, Universidad Autónoma de San Luis Potosí  
México*

### 1. Introduction

In this research we investigate hybrid materials based on Zn-Al alloys near eutectic composition. Two kinds of composite materials were studied bimetallic sheet and particle reinforced Zn-Al-Cu alloys. The particles used were ceramics and intermetallics. The bimetallic is produced by a process comprising providing a strip or sheet of a zinc alloy core and creating a strip or sheet of composite material by metallurgically bonding commercially pure aluminum cladding layers to the zinc alloy. Particle reinforced metal matrix composites were prepared using zinalco as metal matrix by means of powder metallurgy techniques. Alumina, graphite and intermetallic particles were used as reinforcement. The composites prepared using this technique exhibit good consolidation even before sintering. Samples of the base alloy and of the different composites were sintered in air at 473 K in periods of 10, 20, 40 and 80 h. Measurements of density, hardness and yield strength in compression were performed on green and sintered materials. A decrease of 30% in density is achieved for the 27 vol.% alumina composite as compared with the unreinforced base alloy. An improvement of 13% in the values of conventional yield strength and hardness is shown for the composite with 7 vol.% alumina. Metal matrix composites have now been extensively studied, and much of the research concerns the way in which the reinforcing element is added. In some cases ceramic or intermetallic particles are used as a reinforcement material. In other cases, cladding techniques produce a bimetallic with better corrosion resistance properties in extreme corrosion environments, and good mechanical properties. In general the composites have excellent specific mechanical properties, such as specific modulus, specific strength, fatigue resistance, high-temperature performance and very good wear resistance, and so on. Discontinuous reinforcement (particulate, chopped and short fiber, whisker, etc.) composites are currently attracting considerable attention in research and application development fields due to their low cost and simple manufacture. On the other hand, most of the reinforced metallic materials show lower plasticity and toughness than those of the metals matrix. This is one of the main limitations to their use in many industrial fields. Thus, more and more researchers and producers begin to be concerned with the plasticity and toughness of these materials. Special efforts have been made to determine the main factors, which influence the materials plasticity, and to estimate the fracture strain of the reinforced materials. From the viewpoint of running safety and reliability, the quantitative evaluation of their plasticity is an important topic for materials workers.

The primary aim of the present study was to investigate the feasibility of the fabrication of foams, composite and bimetallic materials based on the Zn-Al eutectoid alloy. Dense Zn-

22Al alloy is one of the most commonly used materials for studying superplastic behavior. The reason for this lies in the easy production method of fine equiaxial crystal grains by solution treatment in the single-phase region followed by quenching. The equilibrium diagram Al-Zn has been one of the most investigated over a period of more than 80 years. Two types of phase diagrams have been published (Fig.1) for the Al-Zn system; they differ in the presence or absence of the  $\beta$  high temperature phase and two reactions, a monotectoid one at 340 °C and a peritectic one at 443 °C. For many years the possibility of a peritectic reaction in the zinc-aluminum system has been a subject of discussion. Nayak(1973), studied a small portion of the diagram in great detail and discovered anomalies in high temperature lattice parameters. This led to the reinstatement of a very narrow two-phase region ( $\alpha + \beta$ ) at 72 mass % Zn. The cell parameter of  $\beta$  (ZnAl) phase at 340°C decrease from 0.404 nm at 70 mass% Zn to 0.403 nm at 76mass% Zn. Our recent high-temperature X-ray investigation carried out on  $\beta$  phase, at the composition 78,2 mass%Zn, shows on the diffraction peaks the presence of extra reflections. The analysis shows that the structure corresponds to a triclinic structure. The structure transition from f.c.c (aluminum solid solution at high temperature) to triclinic could be originated by a weak distortion of the cubic phase when the Zn content reaches 70,6 mass%Zn. When this occurs the primitive rhombohedral unit cell ( $a = 285,671$  pm;  $\alpha = 60^\circ$ ) of the f.c.c structure is also distorted, originating a triclinic cell. Our measured triclinic cell parameters are:  $a = 405,057$  pm,  $b = 403,466$  pm,  $c = 403,437$  pm and  $\alpha = 90,22^\circ$ ,  $\beta = 89,99^\circ$ ,  $\gamma = 90,23^\circ$ . The new triclinic unit cell originates on the distortion of the rhombohedral primitive cell contained in this distorted high temperature f.c.c structure. If the  $\beta$  phase is accepted as an intermetallic, the diagram of Fig. 1b accounts for all the experimental facts. In this diagram the invariant transformations in solidification are : a peritectic,  $liq + Al \rightarrow ZnAl(\beta)$ , at approximate 70%Zn, 443°C; and a eutectic ,  $liq. \rightarrow Al(\alpha) + ZnAl(\beta)$  at 94.9%Zn, 382°C. At 275°C it decomposes by an eutectoid reaction into  $Al(\alpha) + Zn(\eta)$  with the eutectoid point at 78%Zn. It is important to realize that the properties of Zn-Al eutectoid alloy, like those of steel, vary with heat treatment. The alloy is put in the superplastic condition, by heating between 280 and 350°C and water quenching. This treatment produces fine grains of  $\alpha$  and  $\eta$  phases. Under this condition, it is capable of severe elongations in excess of 2000% at 250°C.

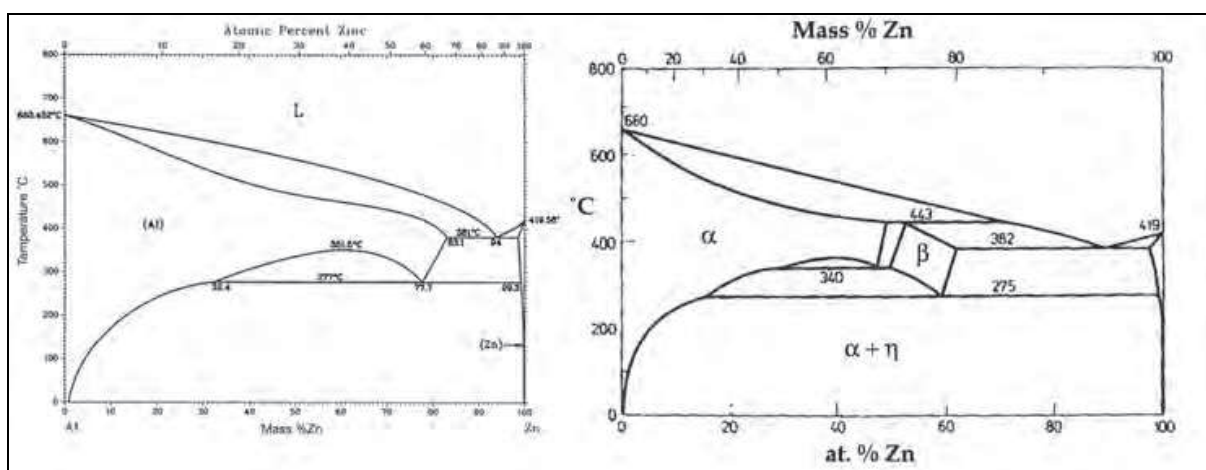


Fig. 1. Zn-Al phase diagrams

The microstructure consists of extremely fine grains (2-5  $\mu\text{m}$ ), which are produced by a cellular transformation, which are almost unresolvable except by electron microscopy. Slowly cooling to room temperature, a pearlitic structure, similar to that of pearlite in steel (Fig.2) is produced

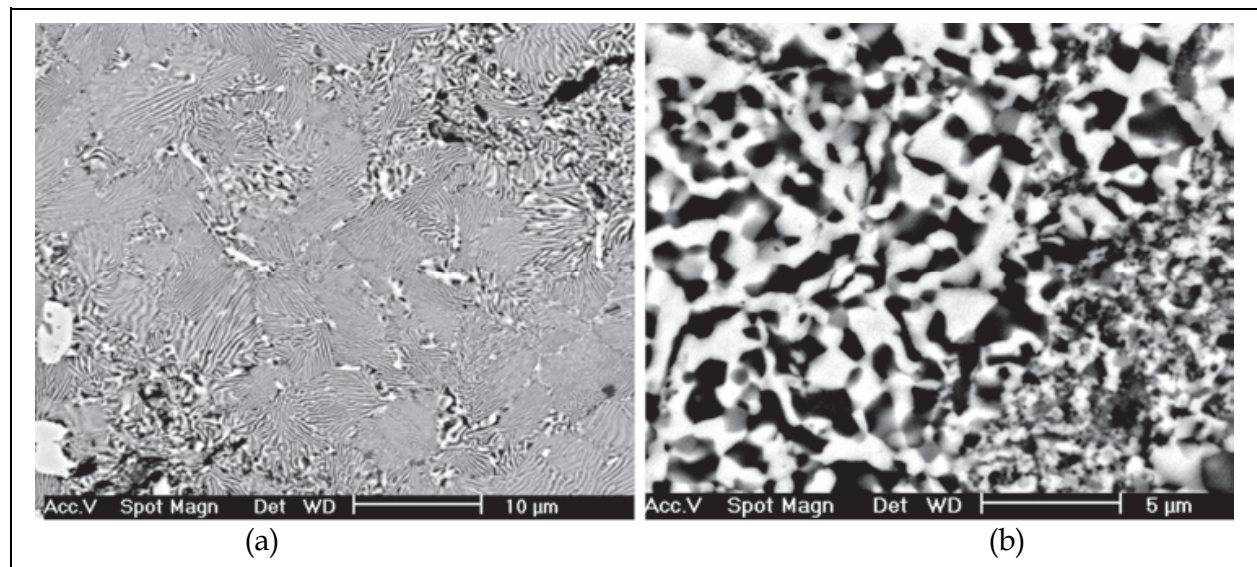


Fig. 2. Microstructures in Zn-Al-Cu. (a) Slowly cooled alloy. (b) Quenched alloy

The addition of copper to the Zn-Al alloy increases the strength and the creep resistance without seriously affecting the superplasticity. Several gravity casting alloys with different copper contents was developed by the international Lead and Zinc Research Organization (ILZRO); they were introduced into the market with the names ZA-8, ZA-12 and ZA-27, the number indicates the amount of aluminum of the alloy. In all cases Magnesium is part of the composition and because of that, the superplasticity is avoided in these alloys. The alloy Zn-20 mass %Al- 2 mass %Cu (zinalco) is an alloy with good properties for gravity casting and in addition it can be rolled and extruded. Copper originates new intermetallic phases at high and low temperatures ( $\epsilon$  and  $t'$ ), which undergo time dependent transformations into equilibrium phases. The zinalco alloy is also unstable at room temperature and transforms by a solid state reaction into a room temperature stable compound containing  $\alpha$  (Al solid solution),  $\eta$  (Zn solid solution) and  $t'$  ( $\text{Al}_4\text{Cu}_3\text{Zn}$ ). However, the reactions take place extremely slowly at room temperature and at a rapidly increased rate as the temperature is raised or by thermo-mechanical treatments i.e. rolling or extrusion. The tensile properties, impact resistance and hardness are all affected by these changes. Furthermore, since some reactions are accompanied by volumetric changes, castings will undergo slight but measurable dimensional changes. The physical and mechanical properties of the zinalco alloy are shown in Tables 1 and 2, it is a high-strength material with engineering properties comparable, in most instances, to those of structural steel and heat-treated aluminum alloys.

Density ( $\text{g}/\text{cm}^3$ )	Melting range ( $^\circ\text{C}$ )	Elastic Modulus (GPa)
5,3 $\text{g}/\text{cm}^3$	420-480	90

Table 1. Physical properties of Zn-20mass%Al-2mass%Cu.

	Yield Strength (MPa)	UTS (MPa)	Elongation (%)	Brinell Hardness
As cast	280	300	3-5	83-90
Die Cast	310	320	8-10	107-116
Extruded	320	410	30-35	40-55
Rolled (superplastic)	290	310	80-100	25-30

Table 2. Mechanical Properties (Room Temperature) of Zn-20mass%Al-2mass%Cu.

## 2. Foams

Metallic foams (porous metals with high porosity ranging from 40 to 98 vol%) are constantly developed and growing as new engineering materials. These exceptionally light weighted materials possess unique combinations of properties, such as impact energy absorption capacity, air and water permeability, unusual acoustic properties, low thermal conductivity and good electrical insulating properties. Several of the engineering properties are superior to those of polymeric foams: they are stiffer by an order of magnitude, they have a higher melting point, they dissipate heat efficiently, they possess superior fire resistance and they do not involve toxic fumes in a fire. Their applications include shock and impact absorbers, dust and fluid filters, engine exhaust mufflers, porous electrodes, high-temperature gaskets, heaters and heat exchangers, flame arresters, catalyst supporters, etc. The field of applications of metallic foams is growing steadily. There are many methods available to produce metallic foams ( Davies & Zhen 1983). Kitazono & Takiguchi (2007) have succeeded in developing close cell Zn-22mass%Al eutectoid alloy foams with superplastic structure through the powder metallurgy process. The strain rate sensitivity exponent ( $m > 0.3$ ), classical of a fine grain structure and absorbed energy of Zn-22Al foams are much larger than those of conventional aluminum foams. This may be due to superplastic deformation of the cell walls. The relative low melting point (480°C) of the eutectoid Zn-Al alloy gave advantages either in compacting or in foaming stage. Daodud (2008) succeeded in preparing a foam composite comprising Zn-22 mass%Al eutectoid alloy and Ni-coated fly ash micro-balloons through the stir casting method. The plateau stress of this foam reach as 100 MPa over a region of a 10-60 % strain and with a density of 3,3 g/cm<sup>3</sup>. The damping property of the eutectoid Zn-Al alloy was studied by Sirong et al. (2007) in composite foams reinforced by 10 vol.% SiC, fabricated with the melt foaming route using CaCO<sub>3</sub> blowing agent. The damping properties of this compound were higher than those of the eutectoid alloy. The addition of Al<sub>2</sub>O<sub>3</sub> short fibers to the Zn-22Al foams increases the compressive yield stress and energy absorption capacity (Jiaan 2008). The behavior of internal friction (IF) and relative dynamic modulus (RDM) in a foamed Zn-Al eutectoid alloy was studied by Wei et al (2002). The specimens with macroscopic pores (0,5-1 mm) were prepared in an air pressure infiltration process. The IF peak is of a grain boundary, which is associated with the diffusive flux on a crystalline boundary between the like-phases of Al/Al. Zn-22Al foams, with an open-cell structure fabricated by the replication process using NaCl preform,

with equivalent cell size to salt particle (840- 3900  $\mu\text{m}$  in size), shows a relation between the relative plastic collapse stress and relative density that can be described with Gibson and Ashby's model (Yu et al. 2009). The relative low melting point (480°C) of the eutectoid Zn-Al alloy give advantages either in compacting or in foaming stage, besides it requires less energy for production. Foams based on Zn-20mass%Al-2mass%Cu (zinalco) alloys have been produced by using granules which can be incorporated into the melt. This method produces an interconnected cellular structure or sponge metal by casting metal around granules introduced into the casting mould. These granules can be soluble (but heat-resistant), such as sodium chloride (ordinary table salt), which is later leached out to leave a porous metal. The eutectoid Zn-Al alloy is well known because of its superplastic properties. Copper additions up to 3% maintains the superplastic properties of the alloy and has obvious strain rate sensitivity, i.e. the stress rises rapidly with increasing strain rate deformation. In addition, the alloy with copper and without copper has excellent damping properties, as we can see from figure 3. Zn-20 mass%Al-2 mass%Cu (zinalco) foams containing up to 50 vol% NaCl grains have been successfully produced using the stir casting technique. Salt grains were pre-heated to 450°C in a graphite mould and molten zinalco alloy (650°C) was poured on the preheated salt grains and then stirred for one minute.

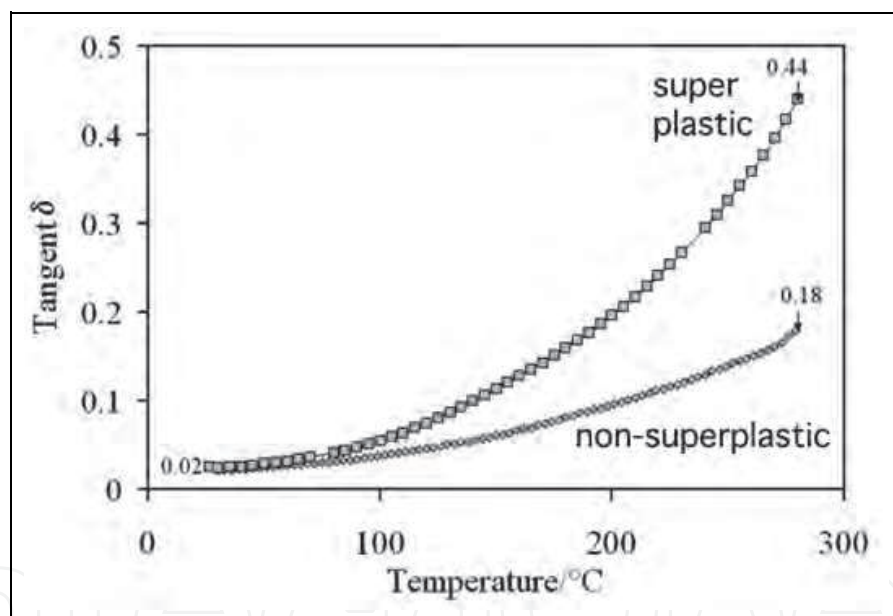


Fig. 3. Dynamical mechanical analysis of the damping behavior ( $\tan \delta$ ), carried out in both superplastic and non-superplastic zinalco.

The mixture was annealed at 450°C for 5 minutes and then furnace cooled. A good wetting between the salt grains and molten zinalco alloy was observed. Figure 4a shows the distribution of the salt grains after solidification, Figure 4b shows the microstructure of the as cast zinalco. It reveals Zn-rich phase ( $\eta$ ) surrounding the dendrites of the aluminum-rich phase ( $\alpha$ ). The light and dark phases in Figure 4b are  $\alpha$  and  $\eta$ -phases, respectively.

The NaCl grains embedded in the metallic matrix were removed washing the specimen with hot water, leaving macroscopic pores in the material and forming foamed specimen. Figure 5. The mean diameter of the macroscopic pores ranges from 2 to 4 mm and a pore volume fraction calculated from:

$$V_f = 1 - (\rho_f / \rho) \times 100$$

where  $V_f$  is the volume fraction of the macroscopic pores,  $\rho$  is the density of dense zinalco ( $\rho = 5,4\text{g/cm}^3$ ) and  $\rho_f$  the measured density of the foam. The calculated pore volume fraction is about 62%. The macroscopic pores are open and with irregular shapes. Two different NaCl crystals sizes (average 4 mm and 1,5 mm) were used which produce two different porous alloys. Type A, with a porous size of  $3 \pm 0,2$  mm with a measured density of  $2 \pm 0,3$  g/cm<sup>2</sup> and Type B with a porous size of  $1,3 \pm 0,3$  mm and a density of  $2,5 \pm 0,2$  g/cm<sup>3</sup>.

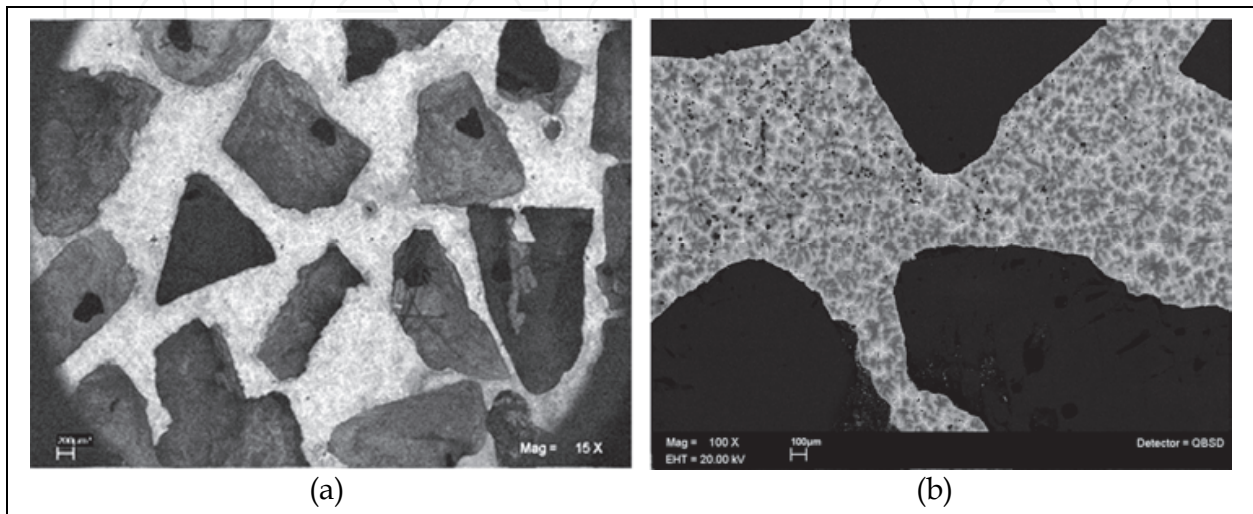


Fig. 4. (a) NaCl grains in a zinalco matrix. (b) Microstructure of the zinalco matrix, in between the NaCl grains

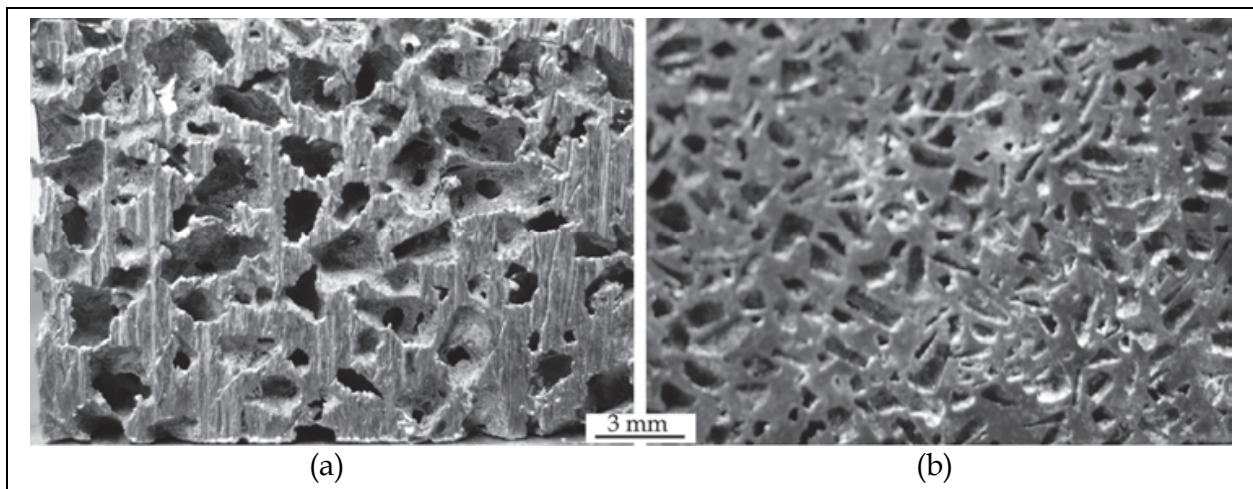


Fig. 5. Images of the porous zinalco alloy produced varying initial salt grain size.

## 2.1 Mechanical properties

Compressive specimens with the dimensions of 15mmx15mmx30mm were prepared from a block of zinalco foam (Fig.5) with a diamond-saw cutting machine. The compressive tests were performed using a universal test Instron machine at a nominal strain rate of  $5 \times 10^{-3} \text{ s}^{-1}$ . Figure 6 shows the compressive stress-strain curves of zinalco foams with different relative

densities. It is found that the stress-strain curves exhibit two distinct regions: a linear elastic region at a very low strain and a plastic plateau region with slight stress fluctuation over a wide range of the strain. Other metallic foams show a third region called the densification region, which was not observed in our zinalco foams, before fracture. The first region is regarded as the elastic bending of cell struts and cell walls (Gibson & Ashby 1997). When the strain reaches about 2%, the failure takes place, and a rapid drop in the stress can be observed after the first peak stress is reached. The collapse stress (defined as the first peak stress) of zinalco foams rises with increasing relative density.

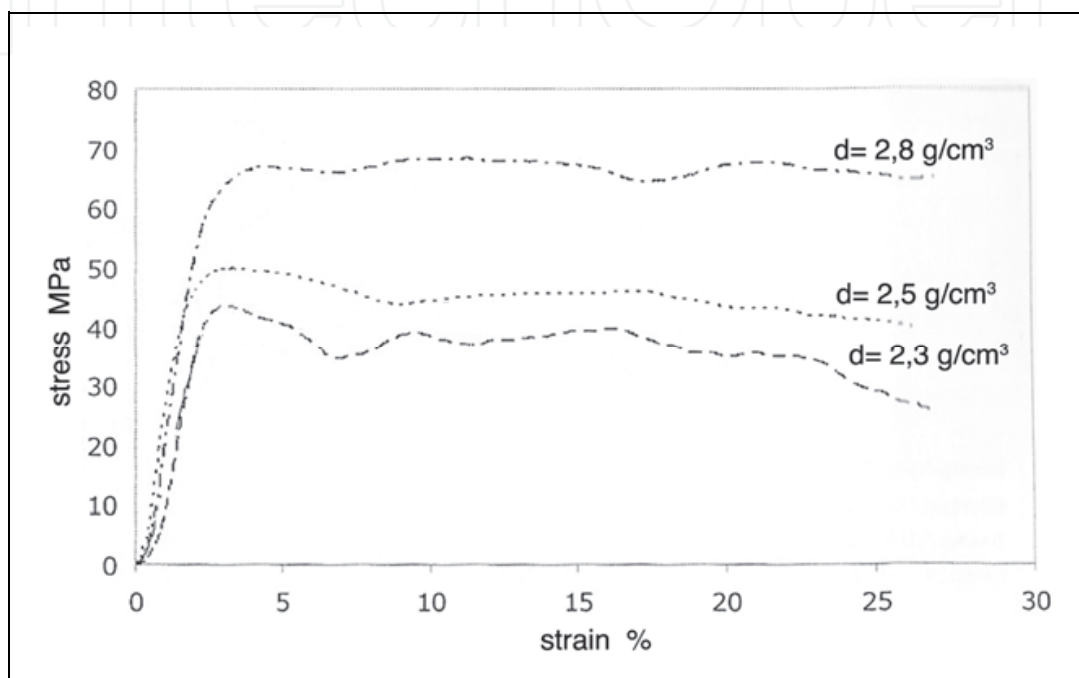


Fig. 6. Compression stress vs. strain for different densities ( $d$ ) of the porous alloy with as cast microstructure.

The microstructure of the zinalco matrix can be changed by thermal treatment. Specimens annealed for 12 hours at 320°C and then water quenched, shows a fine grain microstructure (Fig.2b). This structure induces a higher ductility at room temperature. This thermal treatment has a remarkable effect on the deformation behavior of the zinalco foams. Fig.7. The stress-strain results indicate that the yield stress depends very much on the matrix structure. The foams with the as cast structure shows a higher collapse stress than foam with superplastic structure. This latter material shows a noticeable densification region after a extensive plateau region which is not observed when the matrix has the as-cast structure where a shorter plateau is observed, followed by a rather steep stress increase. A close observation of the deformed specimen with an as cast structure shows that the collapse of the cells takes place on a narrow region at 45° with the load axis (Fig. 8) the rest of the specimen remaining without appreciably deformation. This behavior is probably due to the low ductility (4-5%) of the as cast alloy. In the case of the material with superplastic structure, a uniform deformation is observed.

Figure 9 shows the relationship between the relative plastic collapse stress and relative density for foams with an as-cast structure. The yield stress of the matrix was taken as 280 MPa and the density of the matrix as 5,4 g/cm<sup>3</sup>.

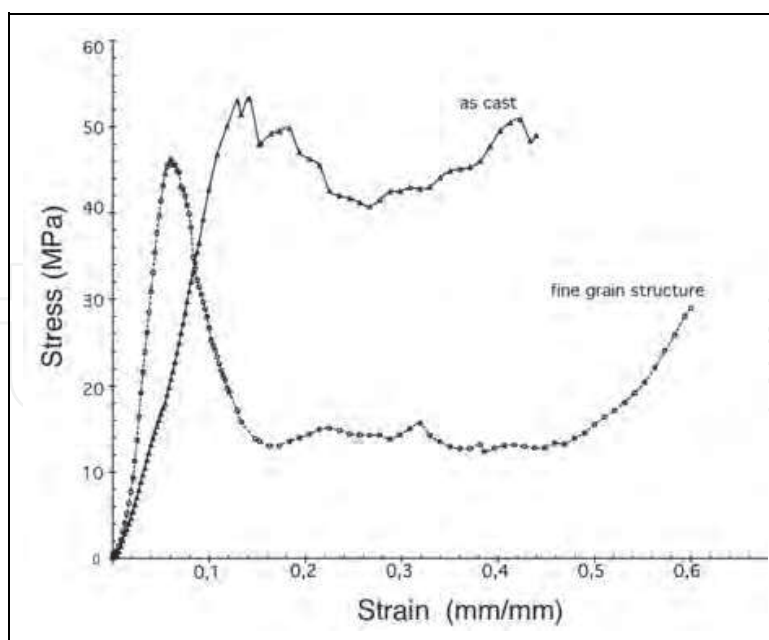


Fig. 7. Compression stress vs. strain behavior of zinalco foams with as cast and fine grain structure.

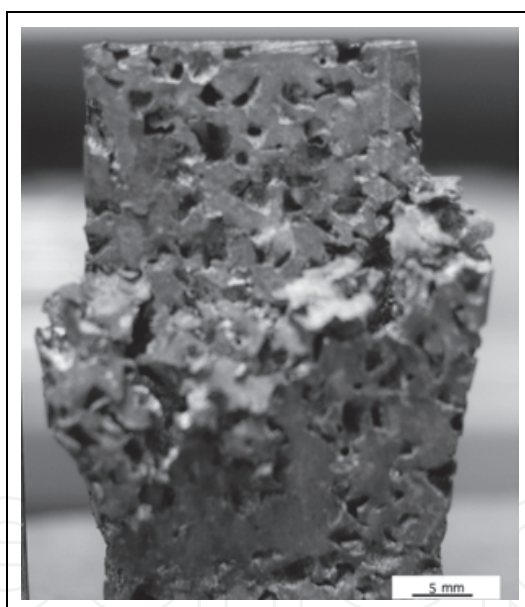


Fig. 8. Localized deformation in zinalco foam with as-cast structure.

Material	Porous size (mm)	Density (g/cm <sup>3</sup> )	Compression stress (MPa)	Energy absorption at 20% strain. (MJ/m <sup>3</sup> )
Foam A	3 ± 0,2	2,8	68 ± 5	3,1 (as cast)
Foam B	2,2 ± 0,2	2,5	48 ± 5	6,5 (as cast)
Foam C	1,5 ± 0,3	2,3	41 ± 3	25 (fine grains)

Table 3. Physical properties of zinalco foams studied in this work.

The plastic collapse stress increases with increasing relative density, in accordance with Gibson and Ashby model.

The energy absorption during the compressive deformation is defined as the energy necessary to deform a given specimen to a specific strain. The energy absorbed per unit volume ( $W$ ) for a sample up to a strain ( $\epsilon_0$ ) can be evaluated by integrating the area under the stress-strain curve. For computing  $W$ , densification strain is taken to be 20%. The mechanical properties of the zinalco alloy foams along with the physical properties are summarized in Table 3. These values are much higher than those observed for low-density aluminum foams. Thus zinalco foams are competitive against the aluminum foams.

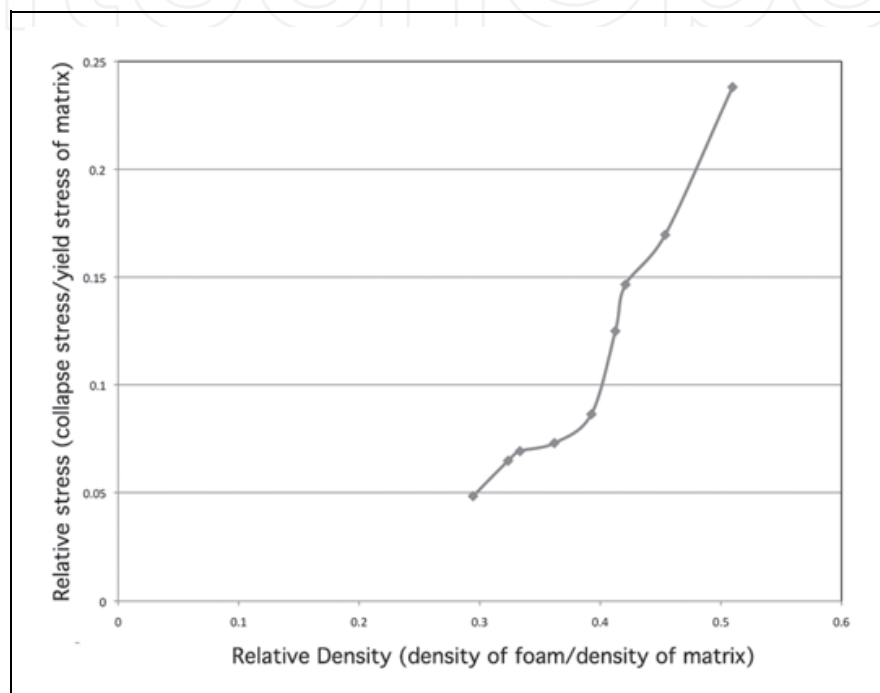


Fig. 9. Variation of the relative stress vs relative density.

### 3. Bimetallic materials

The realization that two metals can be joined together by cladding during rolling or extrusion has gained special importance for heavy metals. Copper sections clad with silver for electrical contacts are produced in this way in a wide variety of shapes. Recently, the plating of copper onto aluminum has been developed. The cladding is usually a layer on each side of the core alloy and usually comprising 2,5 to 5 % of the total thickness. The process requires clean and oxide-free contacting surfaces of the two metals forming the billet to be enlarged during deformation and new surface to be formed. These weld together under the action of the pressure and temperature. The flow stresses of the two metals must be similar (Kwon 2003). The aim of this work is directed to develop an article and a process that satisfy the need for an inexpensive, tarnish resistant, wear resistant, sufficiently hard, composite metal laminate material which is silver in color, does not require secondary annealing and has a composition so that the byproduct of its production process has economic value. The article comprises two commercially pure aluminum-cladding layers metallurgically bonded to a zinc alloy core. The combination of the zinc alloy core and the

commercially pure aluminum cladding layers is ideal for the manufacturing of architectural profiles, keys or coin plachets. The zinc alloy and commercially pure aluminum are inexpensive, silver in color, and sufficiently hard. Zinc and zinc alloys are heavier than the commercially pure aluminum, so that the ratio of each may be adjusted to achieve an acceptable weight for a given application. Further, the tarnish resistance of the commercially pure aluminum cladding layers compensates for the zinc alloy's poor tarnish resistance. The zinc alloys used in the present work are Zn-20mass%Al-2mass%Cu (zinalco) and Zn-22mass%Al-1mass%Ag (zinag). These alloys are high resistant Zn alloys (yield strength  $\approx$  300 MPa.) with a moderate density (5.4 g/cm<sup>3</sup>). Zinalco and zinag alloys, however, are not tarnish resistant. When they are exposed to the atmosphere, the surface of these materials becomes dull gray in color in a relatively short period of time. Because a metallic surface with a dull gray finish is not desirable or marketable, the zinc alloys core is combined with a cladding of aluminum that is tarnish resistant. The core material used in the present work was zinalco and zinag alloy prepared from aluminum and copper of commercial purity. The aluminum cladding layers (upper and lower) are composed of commercially pure aluminum, which is at least about 98,5% aluminum.

Commercially pure aluminum is silvery-white. Further more this aluminum is relatively inexpensive and is of sufficient hardness to ensure a long life and to allow that the products manufactured with it also have excellent resistance to corrosion and tarnishing, providing a long lasting lustrous finish. Besides, commercially pure aluminum is relatively lightweight. Zinag and zinalco alloys billet of 25mm wide, 100mm length and with a thickness of 5mm, were used as core material and aluminum sheet as the sheath material. The initial thickness of sheath material was 0.6mm. The aluminum sheet was fixed at both sides of the billet and then rolled. The range of rolling temperature was varied from 200 to 300 °C ; at this range of temperature zinc alloys shows a strength similar to that of the aluminum strength at this temperature. A thickness reduction of 50% was applied in one pass. After rolling the bonding strength test for the specimens produced under different rolling temperatures was performed. Another simple way to fix the aluminum to the surface of the alloy, was by using thermal spraying and then rolling. This last technique may be an easier way for commercially production of the bimetallic. The cladding thicknesses were from approximately 2% to 3 % of the final sheet thickness (0.4 mm). Tensile test specimens were cut from a composite material composed of Al + Zinag + Al. The samples were tested at 230°C in tension in an Instron universal testing machine at a strain rate of 10<sup>-2</sup> s<sup>-1</sup>. At this strain rate and temperature the zinag alloy hows a maximum deformation of 800%, similar to the zinalco alloy. Figure 10 is a side view of the resultant bimetallic material made of a zinc alloy (zinag) core with two aluminum cladding layers on its opposite sides. The zinag core shows two phases, an aluminum solid solution ( $\alpha$ ) which is dark, and a zinc solid solution ( $\eta$ ) which is bright. Some grains of the  $\eta$  phase are elongated in the direction of the rolling. Zinc diffusion in aluminum is expected to take place during the deformation at 230°C. Figure 11 shows a representative plot of stress (MPa) against strain of the bimetallic material, when tested in tension at 230 °C. A maximum strain obtained in the bimetallic (110%) shows that aluminum non-superplastic can deform superplastically together with superplastic zinalco or zinag. This process is called "membrane forming" (Ward 1988). For the zinalco alloy thicknesses of over 0,5 mm have being formed successfully by this technique during the elongation of the aluminum layer.

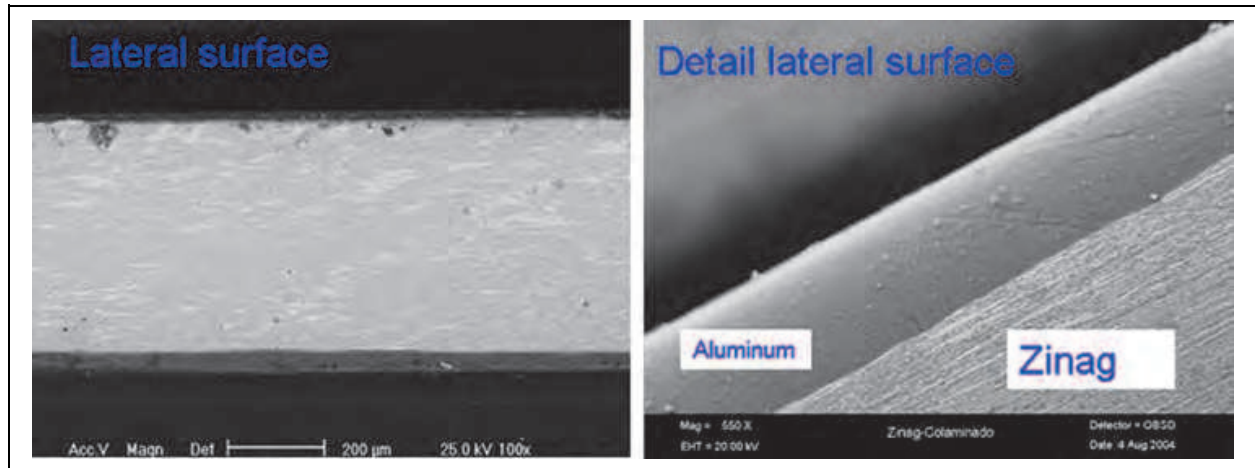


Fig. 10. Lateral view of the bonded Al-zinag-Al alloy interlayer.

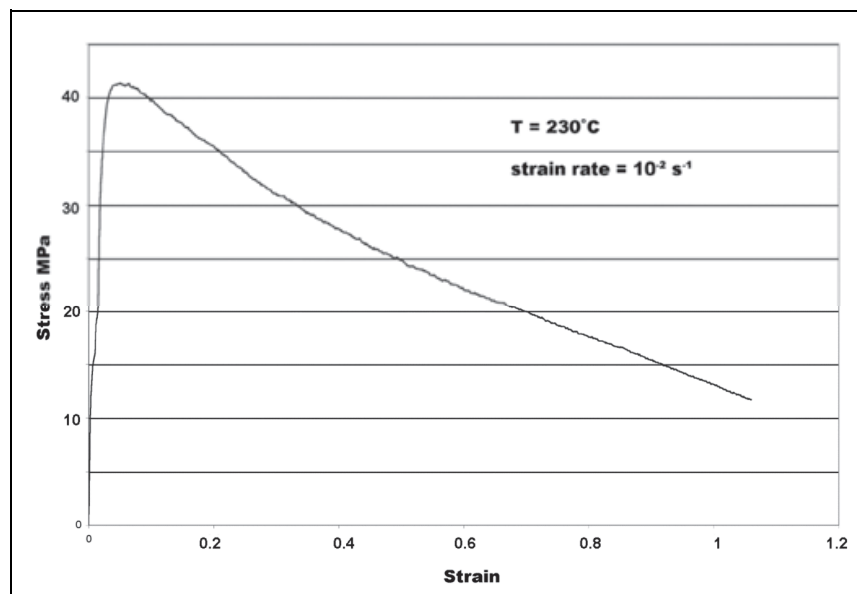


Fig. 11. Stress vs conventional strain tensile diagram of the bimetallic Al-zinag-Al

A detailed examination, of the microstructure of the pure aluminum layer after tensile testing to a strain of 100% at 230°C shows (Fig. 12) elongated chopped grains parallel to the vertical tension axis, imaged by atomic force microscope (AFM). The surface exhibited by the fractured elongated grains is roughly at 45° along the vertical tensile axis. This is known as the plane of maximum shear stresses of the clad material.

These observations can be viewed in figure 13b, in which a scan size of 20 μm was used. As a result of these fractures, the grain size of the aluminum layer is refined during the superplastic forming. In fig 13, a microstructural transversal section zone, typically deformation to both materials is obtained by conventional techniques of vacuum forming for the bimetallic. In the external region of the dome, where tension forces are active a distinctive structure is formed by fine equiaxed grains and black regions, which could be holes. Inspection showed that these round grains are not completely joined together but separated by empty regions. The mechanism of formation of these grains is possible by a fracture of the initial aluminum grains as was observed in the aluminum layer of the

specimens deformed in tension. Figure 12a shows a region where it is possible to observe how a row of grains are fractured on a plane, which is possible at maximum shear stress.

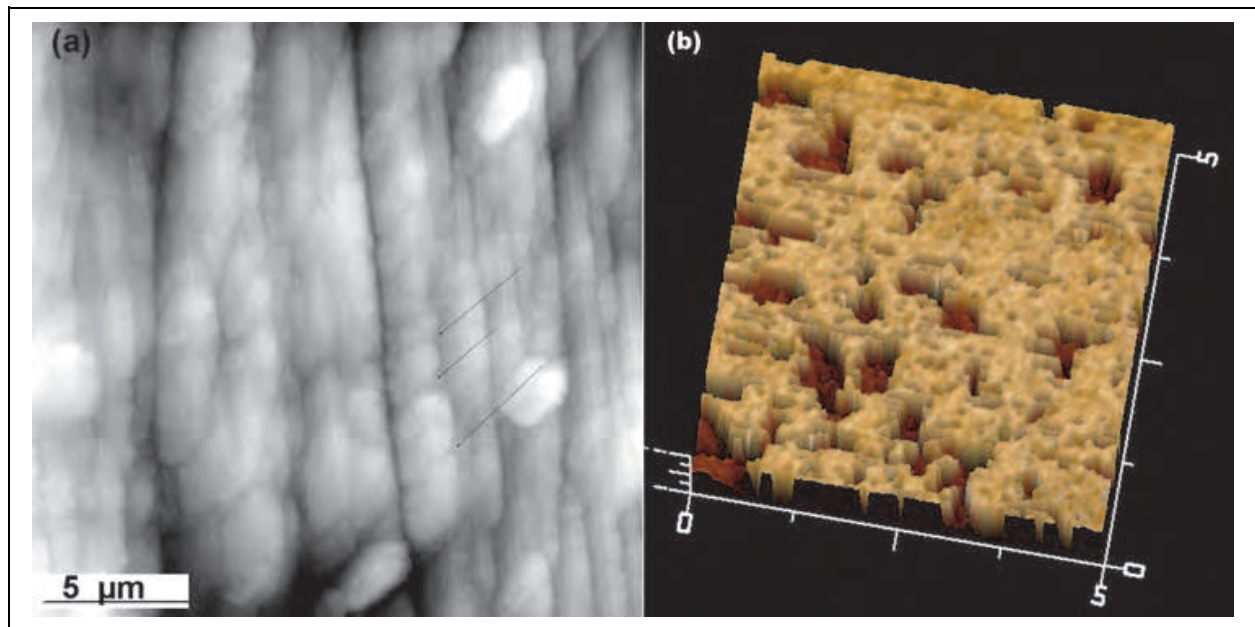


Fig. 12. Topographic view (AFM) of the aluminum layer after tensile deformation.

This plane runs up to the interface zinag-aluminum and then disappears in the superplastic material. Further details about the grains of the deformed discontinuous aluminum layer area are given in figure 12b. At higher magnifications the grains are separated by regions (holes) where new grains are emerging from the lower layers to fill the empty spaces produced when the fractured aluminum grains start to separate. At the boundary between superplastic zinag and aluminum exist a wide band of aluminum-zinc solid solutions, where we do not observe round grains of aluminum. At the initial steps of the deformation of the bimetallic material, the zinag core starts to deform by grain boundary sliding and the aluminum sheath deforms by conventional dislocation mechanisms, which originate work hardening on these grains and elongation in the tension direction. Further deformation fractures of the aluminum grains (shown in Fig.12a) maintain a fine grain structure in this layer. As the deformation proceeds, the superplastic zinag continues deforming by conventional GBS and the aluminum sheath, now composed of a structure of fine grains, starts to deform by GBS originating in the separation of the grains. New grains are emerging (Fig. 12b) from the lower layers to restore the surface. According to the results mentioned above, we consider that the superplastic deformation of the bimetallic material proceeds by a combination of GBS in the superplastic zinag core and an initial conventional deformation in the aluminum layer sheath which elongates the grains in the tension direction. This is followed by a particular superplastic mechanism, produced by the separation of fine grains formed by fractures during the plastic deformation of the elongated aluminum grains. The flow stress of aluminum was 30 to 15 MPa in pure aluminium and 35 to 25 MPa in zinalco or zinag alloy, between 230 °C and 350 °C. Therefore, the flow stress ratio is close to 1 at this temperature range. The required stress to tear out the aluminum sheath from the zinalco's core, is 50MPa when rolling at 240 °C and decreases to 25MPa when rolling is performed at 350 °C (almost the same values for zinag). This suggests that the reducción in strength is due to the phase transformation that takes place in the Zn-alloy core material ( around 275°C)

during the cooling of the bimetallic sheet after rolling, affects the strength of the bonding. The yield strength of this alloy is around 320 MPa. at room temperature; hence the bimetallic Al-zinalco-Al give us a high strength-low density ( $5,2 \text{ g/cm}^3$ ) material, with a great variety of applications in the automotive industry, building and construction or the manufacturing of low cost keys.

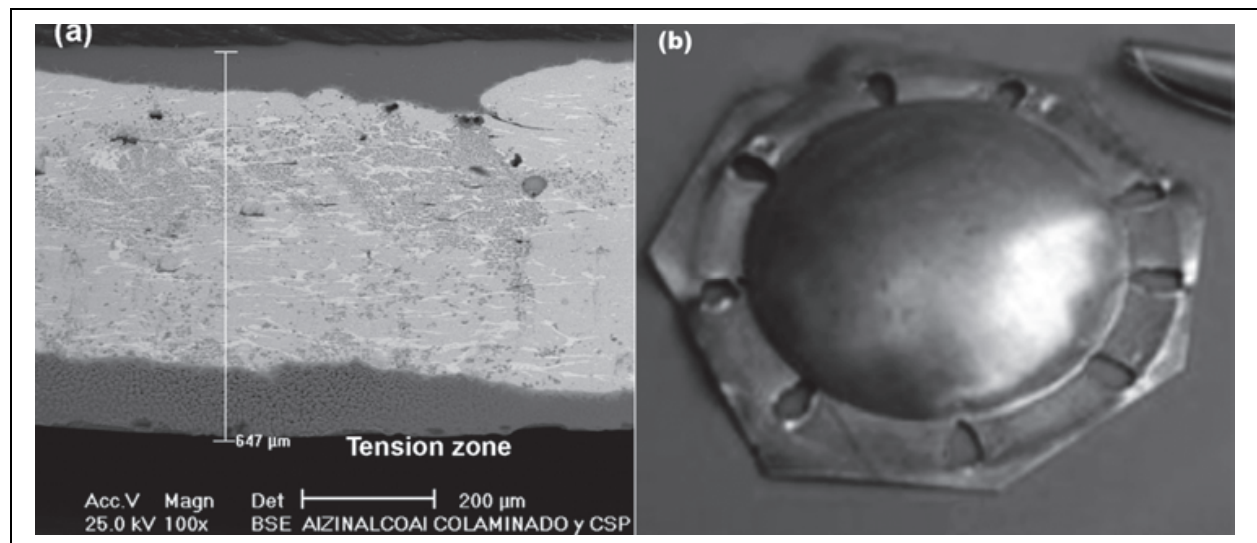


Fig. 13. Transverse section (a) of a dome vacuum formed (b)



Fig. 14. Medals elaborated with aluminum clad zinalco.

The bimetallic zinalco-aluminium is a moderately heavy and soft planchet with excellent applications in the production of coins and tokens. Figure 14 is a top plan view of some products produced with this bimetallic. Scrap may be reused or sold. This economic benefit

is obtained by heating the scrap above its melting point, which produces a zinc-aluminum alloy desired in the die-casting industry. Zinc-aluminum die-cast products are extensively used in the automotive, architectural, aeronautical, and other industries. In this study, the best rolling conditions to obtain an optimum bimetallic planchet were that the rolling temperature was around  $240\text{ }^{\circ}\text{C} \pm 20$  for the alloy Zn-20Al-2Cu. Under this rolling conditions the bonding strength was around  $50\text{MPa}$  for aluminum- zinalco bimetallic planchet.

#### 4. Metal-matrix composites

Composites possess significantly higher strength and stiffness than unreinforced materials zinalco alloy shows very attractive room-temperature properties, these properties decay very rapidly with temperature. Essentially the degradation of tensile strength and creep resistance occurs at temperatures around  $100\text{ }^{\circ}\text{C}$ . With this limitation, the extent of application of the alloy is restricted to those for ambient service temperature environments. An attractive possibility of improving room temperature and relatively high temperature properties ( tensile strength, Young's modulus, wear resistance) is by the reinforcement of particles to form a composite material. Powder metallurgy is a suitable process to produce materials with highly useful characteristics from metal powder alloy without passing through the melt condition. Powder metallurgy provides important technical support for special shape process, principally for five important groups of materials: (1) particulate composite materials, (2) porous materials, (3) refractory materials, (4) frictionless materials and (5) high resistance material with improved properties. Metal powder used in the production of sintered parts can be characterized by three categories of properties: (a) metallurgical properties; (b) geometrical properties and (c) mechanical properties. All these powder properties are the result of the process by which the powder was produced. Parameters like microstructure and chemical composition of metallic powder have a great influence upon the final strength properties of the sintered parts. Impurities may have an adverse effect upon compressibility and upon the life of compacting parts. Particle size distribution, particle shape and particle porosity, determine the powder's specific surface which is the driving force of the sintering process and is directly related to compressibility. The compressibility of the powder is a fundamental factor in deciding the compacting pressure required to achieve a desired compact density. Some advantages in the use of powder metallurgy techniques are: (a) they allow the problems of wet between liquid metal and reinforced ceramic to be overcome, (b) better homogenization of composite materials, (c) high amount of reinforced particles will be attained, (d) a good control of particle size will be obtained, (e) parts with very simple form or with intricate shapes can be easily processed and sintered. Some disadvantages of this technique are: (a) they can be used only for material composites reinforced with particles, (b) the size of parts that can be formed are limited by technique and economic aspects. The forming of particulate material composites using powder metallurgy begins with the mixing of metal and ceramic particles. Powder mixes are compacted in a rigid die. In this operation, high pressure (about  $650\text{ MPa}$ ) is exerted upon the powder in the die cavity using one or more vertically moving compacting punches. Under the influence of such high compacting pressures, the powder particles are being squeezed together so closely that their surface irregularities interlock and a certain

amount of cold welding takes place between their surfaces. The compaction process does not require high temperature, it can be performed at room temperature, therefore, there is low interaction between metal and reinforce particles, minimizing undesirable interfacial reactions to get better mechanical properties. This investigation examines the properties of Zinalco matrix combined with alumina, graphite, hidroxiapatite and intermetallic particles, fabricated by conventional cold powder pressing and hot solid state sintering techniques. In general, the goal of grinding could be: (a) to diminish the size of particles, (b) to mix the powder of raw material or (c) to study microstructural and morphology changes.

#### 4.1 Characterization of reinforcement particles

Filings of Zinalco alloy were comminuted in a vibratory milling and in a high-energy planetary mill. The resultant particles are shown in figure 15.

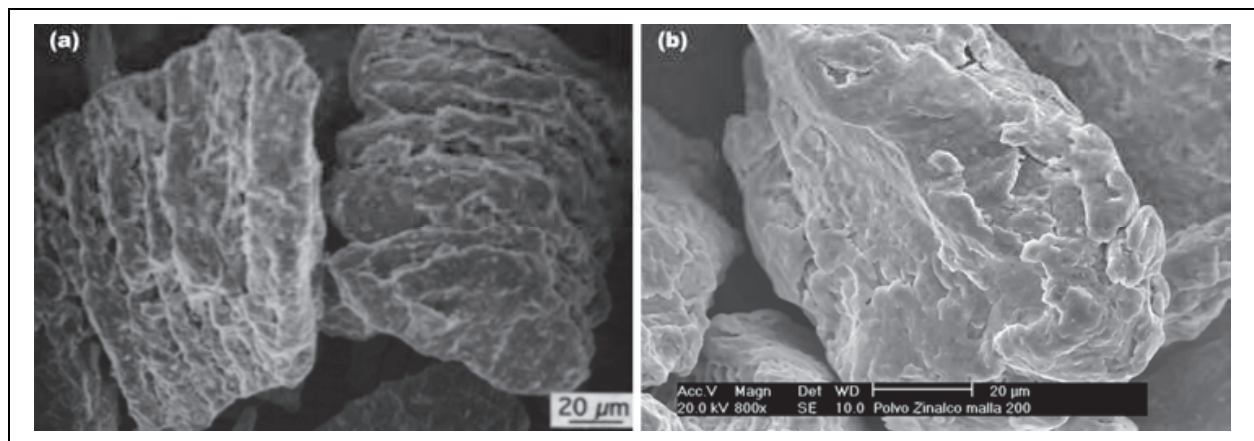


Fig. 15. (a) Zinalco powder obtained with a vibratory mill has flake shape and a groove surface, (b) rounded particles of zinalco powder obtained in a high energy planetary mill.

Figure 15a shows powder obtained by this process the particles have a flake shape with a grooved surface. Figure 15b, shows rounded shape powder obtained when a cast-alloy comminuted in a high energy planetary mill. Particle surface shows intense plastic deformation and grooves are less deep than particles obtained in the vibratory mill. Fig 16a shows the microstructure of the cold compacted powder, there can be observed  $\alpha$  (black) and  $\eta$  (brighth) fine grains. X ray diffraction pattern of this material still shows the presence of the metastable  $\epsilon$  phase. Powder obtained in vibratory mill, requires long periods of grinding, about 100 hours, for total  $\epsilon$  phase transformation into the  $\tau'$  phase, which is the stable phase at room temperature. Cold compacted zinalco powder was sintered at 200°C in air; the average size of equiaxed grains before sintering was 800 nm. After long periods of sintering, about 20 hours or more, the microstructure transformed into interconnected grains and an important increase in size was observed; see figure 16b. Both zinalco grinding processes, were performed without any protective atmosphere, unlike other powder metals such as aluminum and magnesium that can be explosive and require inert atmosphere. The x-ray diffraction pattern of both zinalco alloys compacted powder does not show reflections related to the presence of zinc oxide or aluminum oxide; this indicate that material do not present an appreciable oxidation. Ceramic particles as reinforce of metal matrix composites give the opportunity of combine the relative easily capacity of metals and alloys for

deformation with the hardness, high strength and low density of ceramic particles. In the first stage of this work it was studied three different kinds of reinforce particles were studied. The first one was  $\gamma$ -alumina powder of commercial distribution with average particle size of 0.05  $\mu\text{m}$ . average diameter.

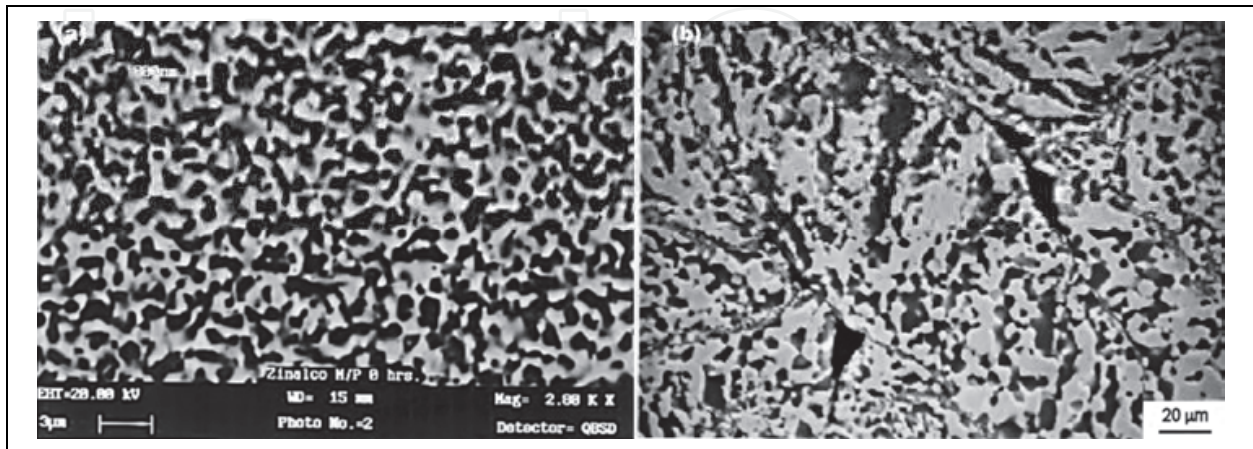


Fig. 16. (a) Microstructure of Zinalco flakes cold compacted . (b)Microstructure of zinalco compacts sintering at 473K during 80 hour in air atmosphere.

This material has been widely used to reinforce composites based on aluminum alloys, principally to improve its temperature resistance and to increase its tensile strength. In Zinalco-alumina composites we attempt to diminish the density of this material and improve its compression strength. Alumina particles gathered to form clusters with 10  $\mu\text{m}$  eliminate. Graphite form plates or thin sheets eliminate these plates has a wide size distribution from 0,05  $\mu\text{m}$  up to about 25  $\mu\text{m}$ . Density of this material was 2.26  $\text{g}/\text{cm}^3$ . The graphite presumably imparts improved tribological properties to the composites through the formation of a graphite-rich film on the tribo-surface which provides solid lubrication (Rohatgi 1992). Hidroxiapatite powder [ $\text{Ca}_{10}(\text{PO}_4)_6(\text{OH})_2$ ] forms clusters with a wide size distribution as shown y figure 17a. This is a crystalline material with applications as biomaterial. In a second stage of this work, it was used to reinforce reinforced the intermetallic 57mass%Cu-26mass%Al-17mass%Zn (phase t'). Ingots of as cast intermetallic were comminuted in a bar mill to form particles of about 1 mm diameter and then refined in a n horizontal ball mill until a size distribution between 30 and 45  $\mu\text{m}$  was obtained, as show in figure 17b. The formation of a compound using powder metallurgy starts with a compaction process and then green compacts are subjected to a densification process. Regular compaction process are: (a) to apply pressure into a rigid die, (b) to apply isostatic pressure into a flexible mould, (c) rolling compaction of powder and (d) powder extrusion. For compaction it is necessary to apply higher pressures, about 650 MPa. In this work zinalco-ceramic composites were prepared by uniaxial compaction into a rigid die at room temperature while zinalco-t' composites were formed by both hot extrusion and hot forging process of the powder material. Physical and mechanical properties of composites material depends on homogenous mixture of powder raw materials. In all cases materials were manually mixed and then blended in a mechanical mill.

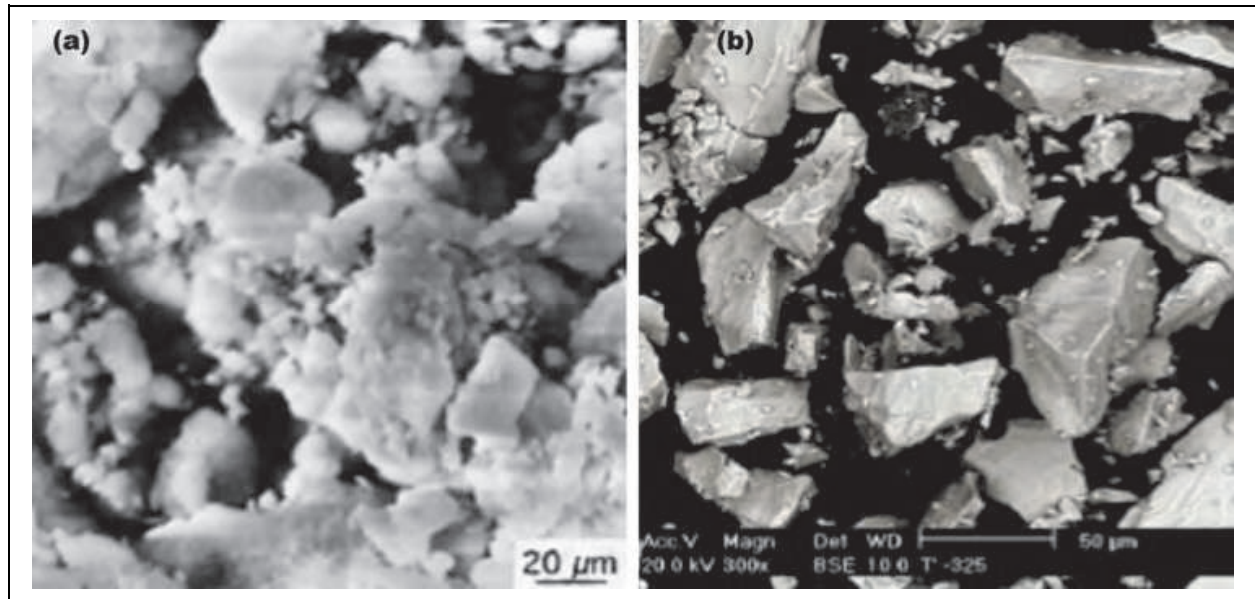


Fig. 17. (a) Clusters of hidroxiapatite. (b) Particles of intermetallic  $\tau'$  used as reinforce.

For the uniaxial compaction of powder it is important to control die filling, frictional conditions, and velocity range of load application. After the compaction process it is necessary to determine the temperature and time of sintering. Forging and extrusion processes were performed at 250 °C, at which temperature we found less porosity and higher hardness. Using powder metallurgy techniques zinalco-alumina, zinalco-graphite and zinalco-hidroxiapatite composites were prepared. A maximum of 20 mass% of alumina, 20 mass% of graphite and 15 mass% of hidroxiapatite were incorporated in the composites. Composites with 5 mass% alumina, 7 mass% graphite and 5 mass% hidroxiapatite show good mechanical characteristics. In all composites were observed a homogeneous distribution of reinforced particles. With other methods of preparation such as reocasting only a maximum of 1,2 mass% of alumina and 3 mass% of graphite could be incorporated (Muñoz-Lasso, 1992). In these composites it was observed that reinforced particles were not homogeneously distributed into the metal matrix and formed clusters. Zinalco- $\tau'$  compounds were prepared by hot forging; a maximum of 50 mass%  $\tau'$  was incorporated. Figure 18a shows the microstructure of zinalco-10 mass%  $\tau'$  hot-forged material. The microstructure of the extruded material is formed by equiaxed grains and a preferential orientation in direction of extrusion is observed see figure 18b. An advantage of adding ceramic particles into a metallic matrix is to diminish the density of the resulting material. Table 4 shows the results of the density changes that occur after sintering the pure and reinforced alloy. The theoretical values were calculated using mixture rules. The actual density for the composites prepared under conditions of this work changes from 5,0 g/cm<sup>3</sup>, for unreinforced material, to 3,83 g/cm<sup>3</sup>, for composite with 27 vol. % alumina. This large change observed in density, is due to porosity as well as the large amounts of alumina. No appreciable volume changes were observed during the sintering of these composites, density remained almost constant for all compositions and sintering time. At the sintering temperature used in this paper ( 200 °C) there was not expected any bonding between ceramic particles. Zinalco composite reinforced with 10 wt. %  $\tau'$  has an average density of 5,17 g/cm<sup>3</sup> in both hot-forging and hot-extruded materials.

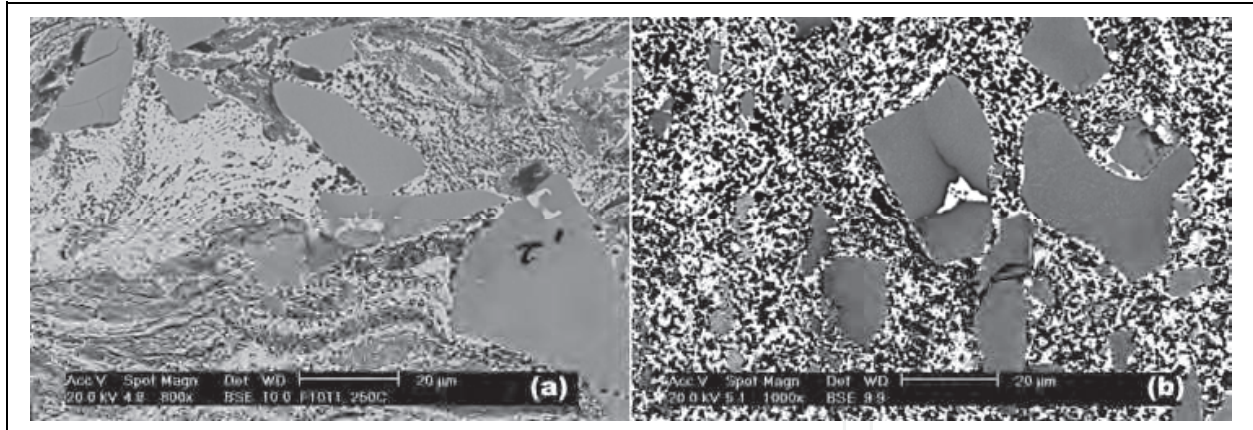


Fig. 18. (a) Zinalco 10 mass% $\tau'$  forged at 523 K in air, the alloy retains as-cast microstructure. Zinalco 10 mass% $\tau'$ , extruded at 523 K in air, zinalco base alloy show equiaxed grains of  $\alpha$  and  $\beta$  phases.

#### 4.2 Mechanical properties

The base alloy yield stress in compression was measured in both green and sintered material. The compressive properties of ceramic composites tested in function of the sintering time are shown in figure 19. Results indicate that addition of 5 wt.% alumina particles into the zinalco matrix cause an improvement of the yield strength after sintering, reaching an increment of 13 %in yield stress after 20 hours of sintering. Yield strength remains almost constant for longer sintering times in all tests. Composites with 10 and 20 wt. % alumina and with 7 wt. % graphite fracture without yielding. Hardness (Fig. 20) diminishes when alumina content is 20 wt. % because a great amount of unsintered ceramic particles separates more easily when the load is applied. Hardness increases with sintering time for the unreinforced base alloy, for zinalco-5 wt.% hidroxiapatite and zinalco-5 wt.% alumina composites, hardness reach a maximum after 20 h of sintering time, then the hardness remains almost constant.

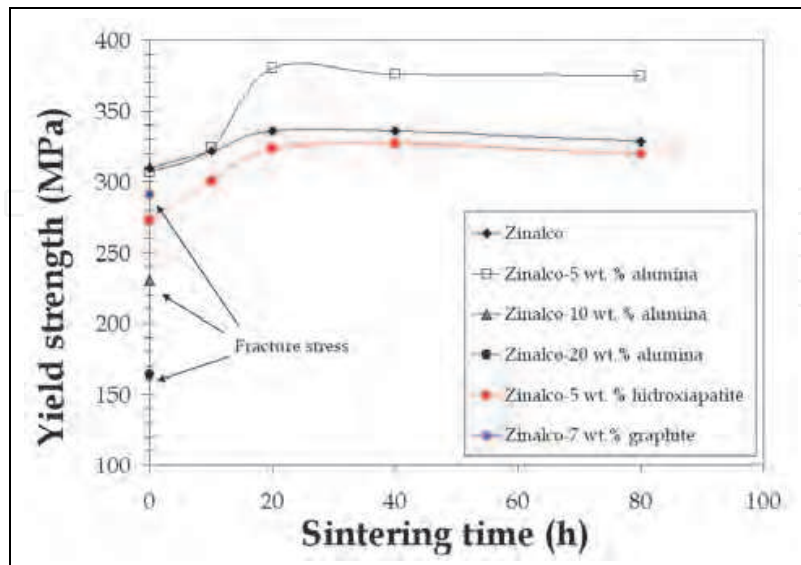


Fig. 19. Effect of sintering time on yield strength of zinalco, zinalco-alumina composites, zinalco-5 mass% hidroxiapatite and zinalco-7 mass% graphite. Tests were performed at strain rate  $10^{-3} \text{ s}^{-1}$ .

Material	Density (g/cm <sup>3</sup> )		Porosity (%)
	Theoretical	Actual	
Zinalco	5,40	5.00	7
Zinalco-5 mass% alumina	4,92	4,51	8
Zinalco-10 mass% alumina	5,15	4,44	14
Zinalco-20 mass% alumina	4,91	3,83	22
Zinalco-7 mass% graphite	4,63	4,43	4
Zinalco-5 mas% hidroxiapatite	4,85	4,57	6
Zinalco-10 mass% $\tau'$ hot forging	5,56	5,18	7
Zinalco-10 mass% $\tau'$ hot extruded	5,56	516	7

Table 4. Theoretical and actual density for zinalco-ceramic composites sintered 10 h at 473 K and zinalco 10 mass% $\tau'$  obtained by both hot forging and hot-extrusion at 523 K.

The hardness of the zinalco-7wt. % graphite composite remains almost constant with sintering time. Studies of the effect of strain rate over the mechanical properties were undertaken for zinalco-alumina composites, (Fig.21). Reinforced material with 5 wt. % alumina increases its ductility up to  $10^{-3} \text{ s}^{-1}$  and then starts to fail in a brittle manner. Green unreinforced zinalco behaves in a way similar to high strain rate superplastic metals (Nieh et al., 1984) reaching 113% of true strain at  $10^{-1} \text{ s}^{-1}$  and it may be possible to reach higher values at a higher strain rate, not measured in this work, (Fig.21b). This behavior changes completely with long sintering periods and maximum deformation achieved is lower in unreinforced and reinforced zinalco tested at any strain rate. Figure 23 shows the microstructure of green composite with 5 wt.% alumina deformed 113% in compression. It is possible to observe a plastic deformation of metal particles, which are elongated perpendicularly with respect to the compression axis. Metal particles slip one over the other because the alumina interface has been broken into small rounded pieces. The sintering process produces welding between metal particles and makes the boundary slip more difficult, reducing the ductility of this material. Composites with 10 and 30 mass%  $\tau'$  hot extruded and unreinforced hot extruded zinalco base alloy were tested in compression using two values of strain rate of  $10^{-2}$  and  $10^{-1} \text{ s}^{-1}$ . Table 5 summarized yield stress values and hardness Rockwell B values for these materials

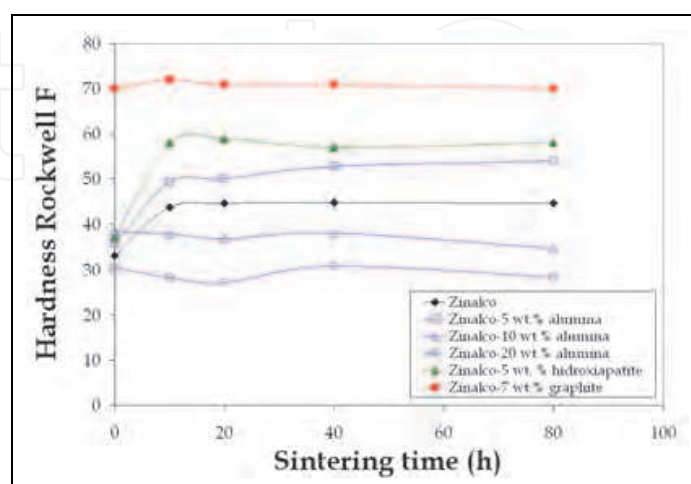


Fig. 20. Effect of sintering time on hardness of zinalco unreinforced base alloy and zinalco-ceramic composites.

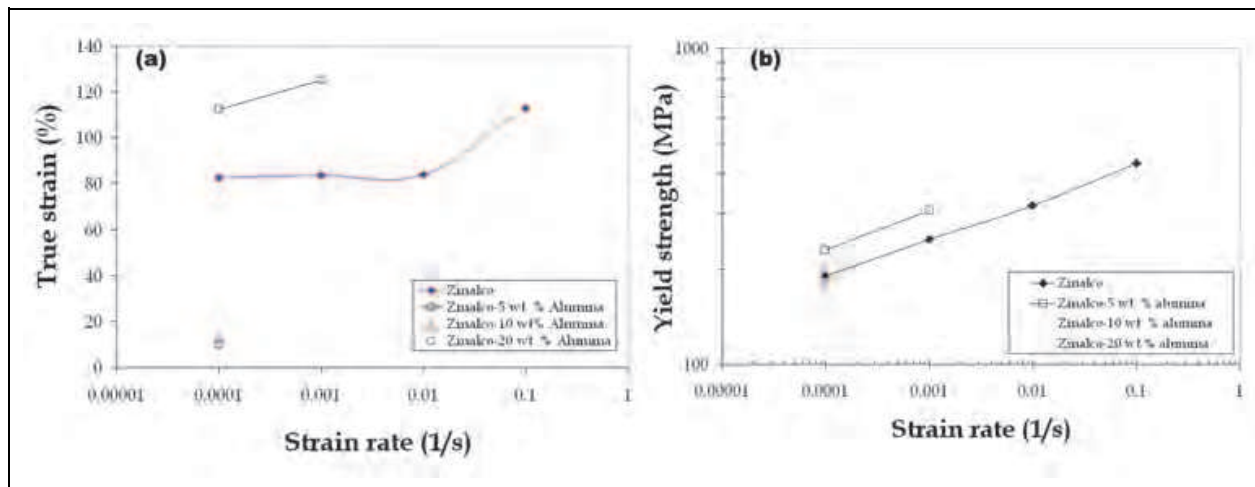


Fig. 21. Effect of strain rate on (a) yield strength and (b) true strain for zinalco unreinforced base alloy and zinalco-alumina green composites.

Hot extruded Material	Yield stress (MPa)	Yield stress (MPa)	HRB
	$\dot{\epsilon} = 10^{-2} s^{-1}$	$\dot{\epsilon} = 10^{-1} s^{-1}$	
Zinalco	238,3	252,8	32,17
Zinalco- 10 wt. % t'	238,8	253,8	38,92
Zinalco- 30 wt. % t'	291,0	189,7	60,92

Table 5. Yield stress values for hot extruded composite materials and unreinforced base alloy

### 4.3 Conclusions

The incorporation of ceramic and intermetallic particles in zinalco alloy modifies density and mechanical properties with respect to the unreinforced alloy. The low sintering temperature (200 °C ) used in this work is not enough to produce sintering of ceramic particles, therefore under these experimental conditions, large amounts of ceramic reinforce produce brittle behavior and eliminate grain growth inside metal particles. During mixing and compaction operations, fine ceramic particles infiltrate into groves on the zinalco filling surface, making a smoother interface, resulting in a better accommodation of the distorted particles during deformation at low strain rates ( $< 10^{-3} s^{-1}$ ) in 5 mass% alumina unsintered composite and increasing total strain with respect to the unreinforced green zinalco alloy, see figure 22b. In green base alloy a linear dependence of yield stress with the strain rate was observed see figure 22(a). These values increase as function of strain rate. This behavior changes with sintering process in reinforced and unreinforced materials. In the sintered ones yield stress was observed only when the strain rate was below  $10^{-3} s^{-1}$ ; for higher strain rates ( $>10^{-3} s^{-1}$ ) fracture occurs without yielding in both sintered materials, possibly due to the diffusion bonding between metal particles, which obstructs the free accommodation of these particles one over the other. Yield strength in the unreinforced material achieves a maximum after 20 hours of sintering and then the stress remains constant with longer sintering time. In reinforced material with 5 mass% alumina yield stress increases up to 20 hours. The initial increase of the yield stress in both reinforced and unreinforced materials is probably due to the diffusion bonding of the metal particles that obstructs the free

accommodation of the deformed metal particles. A bigger yield stress is observed in the case when the alumina is present an increase in alumina weight fraction (10 and 20 mass.%), results in a poor contact between metal particles, reducing the possibility that diffusion bonding can occur between them and hence the material behaves in a very brittle manner because particle/alumina decohesion occurs. Composites reinforced with  $\tau'$  intermetallic particles were formed by hot-forging and hot extrusion process. Better mechanical properties were observed in the as-extruded composite because the microstructure consists of equiaxed grains produced by severe plastic deformation. It can be very interesting to study if superplasticity at high strain rates ( $>10^{-1}$ ) can be achieved with powder metallurgy in Zn-Al alloys.

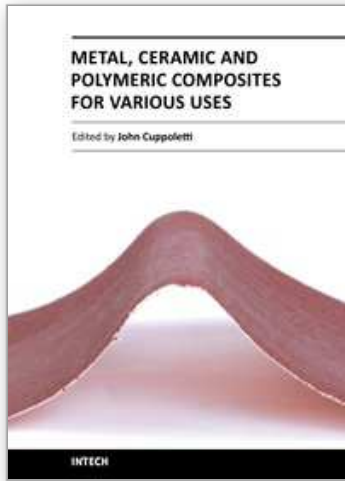
## 5. References

- Davies G.J. & Zhen S. (1983). Metallic foams: their production, properties and applications. *Journal of Materials Science* Vol.18, No. 4 (July 1983) pp1899-1911, ISSN 1573-4803.
- Daoud A. (2008). Synthesis and characterization of novel ZnAl22 syntactic foam composites via casting. *Materials Science and Engineering A* Vol.488, (2008), pp. 281-295
- Gibson L.J. & M.F. Ashby M.F.(1997). Cellular Solids: Structure and Properties (2<sup>nd</sup> ed) Cambridge University Press, Cambridge, UK (1997)
- Kwon H.C., Jung T.K., Lim S.C. & Kim M.S..(2003) "Fabrication of copper clad aluminium wire" *Designing, Processing and Properties of Advanced Engineering Materials*, Korea 2003, Trans Tech Publications LTD pp 317-320.
- Jiaan L., Sirong Y., Xianyong Z. Ming W., Song L., Yanru L. & Yaohui L. (2008) Effect of Al<sub>2</sub>O<sub>3</sub> short fiber on the compressive properties of Zn-22Al foams. *Materials Letters* Vol. 62 (2008), pp 3636-3638
- Kitazono K & Takiguchi Y. (2007). Strain rate sensitivity and energy absorption of Zn-22Al foams *Scripta Mater.* Vol.55 (2006),pp. 501-504
- Muñoz-Lasso A. (1992). Estudio de las propiedades mecánicas de un compuesto con matriz metálica (Zinalco). *Tesis de Maestría en Ciencias*. Facultad de Ciencias. UNAM. México 1992.
- Nayak A. K. (1973). Thermal and quantitative thermal analysis of Al-Zn alloys and determination of the equilibrium diagram of the binary system. *Journal of the Institute of Metals*. Vol. 101, (1973) pp 309-314.
- Rohatgi P.K., Ray S. & Lin Y.(1992) Tribological properties of metal matrix graphite particle composites. *International Materials Review*. Vol.37, No. 3(1992), pp. 129-135
- Sirong Yu, Jiaan L., Yanru L.& Yaohui L. (2007). Compressive behavior and damping property of ZA22/SiC<sub>p</sub> composite foams. *Materials Science and Engineering A* Vol. 457 (2007), pp325-328.
- Ward D.M. (1988) Forming non-superplastic materials with superplastic membranes. *Proceedings of an International Conference on Superplasticity and Superplastic Forming*, pp. 595-599. ISBN 0-87339-089-X, Blain, Washington, August 1-4,1988.
- Wei J, N., Cheng H.F., Gong Ch, L. Zhou Z. C., Li Z.B., Han F.S. (2002). Grain boundary peak in a foamed Zn-Al Eutectoid alloy. *Chin.Phys.Lett.* Vol.19, No. 3, (2002),pp.381-384.

Yu S., Liu J., Wei M., Luo Y., Zhu X., Liu, Y. (2009). Compressive property and energy absorption characteristics of open-cell ZA22 foams. *Materials and Design*. Vol. 30(2009), pp. 87-90.

IntechOpen

IntechOpen



## **Metal, Ceramic and Polymeric Composites for Various Uses**

Edited by Dr. John Cuppoletti

ISBN 978-953-307-353-8

Hard cover, 684 pages

**Publisher** InTech

**Published online** 20, July, 2011

**Published in print edition** July, 2011

Composite materials, often shortened to composites, are engineered or naturally occurring materials made from two or more constituent materials with significantly different physical or chemical properties which remain separate and distinct at the macroscopic or microscopic scale within the finished structure. The aim of this book is to provide comprehensive reference and text on composite materials and structures. This book will cover aspects of design, production, manufacturing, exploitation and maintenance of composite materials. The scope of the book covers scientific, technological and practical concepts concerning research, development and realization of composites.

### **How to reference**

In order to correctly reference this scholarly work, feel free to copy and paste the following:

Elizabeth Martínez-Flores and Gabriel Torres-Villaseñor (2011). Hybrid Materials Based on Zn-Al Alloys, Metal, Ceramic and Polymeric Composites for Various Uses, Dr. John Cuppoletti (Ed.), ISBN: 978-953-307-353-8, InTech, Available from: <http://www.intechopen.com/books/metal-ceramic-and-polymeric-composites-for-various-uses/hibrid-materials-based-on-zn-al-alloys>

**INTECH**  
open science | open minds

### **InTech Europe**

University Campus STeP Ri  
Slavka Krautzeka 83/A  
51000 Rijeka, Croatia  
Phone: +385 (51) 770 447  
Fax: +385 (51) 686 166  
[www.intechopen.com](http://www.intechopen.com)

### **InTech China**

Unit 405, Office Block, Hotel Equatorial Shanghai  
No.65, Yan An Road (West), Shanghai, 200040, China  
中国上海市延安西路65号上海国际贵都大饭店办公楼405单元  
Phone: +86-21-62489820  
Fax: +86-21-62489821

© 2011 The Author(s). Licensee IntechOpen. This chapter is distributed under the terms of the [Creative Commons Attribution-NonCommercial-ShareAlike-3.0 License](#), which permits use, distribution and reproduction for non-commercial purposes, provided the original is properly cited and derivative works building on this content are distributed under the same license.

IntechOpen

IntechOpen